ELSEVIER

# DFT studies of structures and vibrational spectra of silicon–sulfur clusters $(SiS_2)_n^+$ ($n = 1$–5)

Su-Fan Wang[a], Ji-Kang Feng[a,*], Kun-Qian Yu[a], Meng Cui[a], Ai-Min Ren[a], Chia-Chung Sun[a], Peng Liu[b], Zhen Gao[b], Fan-Aao Kong[b]

[a]*State Key Laboratory of Theoretical and Computational Chemistry, Institute of Theoretical Chemistry, Jilin University, Changchun 130023, People's Republic of China*
[b]*State Key Laboratory of Molecular Dynamics, Institute of Chemistry, Chinese Academy of Science, Beijing 100080, People's Republic of China*

Received 9 April 1999; accepted 23 August 1999

## Abstract

The possible geometrical structures and relative stabilities of silicon–sulfur clusters $(SiS_2)_n^+$ ($n = 1$–5) are explored by means of DFT quantum chemical calculations. The effects of polarization functions and electron correlation are included in these calculations. The electronic structure and vibrational spectra of the most stable geometrical structures on each $(SiS_2)_n^+$ potential energy surface are analyzed by the same method. As the result, the regularity of the $(SiS_2)_n^+$ cluster forming is obtained that is the most stable structure of $SiS_2^+$ is with $D_{\infty h}$ symmetry, and $(SiS_2)_n^+$ ($n = 2$–5) have tetra-atomic rings of Si and S atoms bound alternatively, and the rings are perpendicular to each other. The calculation may predict the mechanism of the $(SiS_2)_n^+$ cluster forming is based on the bonding of Si and S atoms with $SiS_2^+$ as the core and $SiS_2$ as the building block, forming tetratomic ring molecular chain with rings perpendicular to each other. © 2000 Elsevier Science B.V. All rights reserved.

*Keywords*: Silicon–sulfur clusters; Geometry; Electronic structure; Vibrational spectra

## 1. Introduction

The theoretical study of clusters is becoming more and more important with new clusters being synthesized continuously. The research of non-metal clusters have developed widely since fullerene was discovered [1–3]. In particular, the observation of silicon and sulfur clusters attracted much attention.

Silicon is one of the most abundant elements on earth. Its importance in science and technology results from its diverse use ranging from glass to catalysis to Si-based microelectronic devices and optical fiber communications. That is why silicon clusters have been the subjects of a series of experimental and theoretical studies during the last ten years. There are many theoretical studies on silicon clusters recently, ab initio calculations of the properties of silicon clusters have been carried out by several investigators. These calculations have proved to be invaluable in understanding the various experiments carried out on silicon clusters. For example, the geometries and vibrational frequencies of neutral silicon clusters up to $Si_{10}$ were calculated by Raghavachari [4] before any of the above experiments were carried out. This was followed by calculations by Raghavachari and Rohlfing on the geometries and frequencies of negative ions as well as the low-lying excited states for several of the neutral clusters [5]. Moreover, there were many

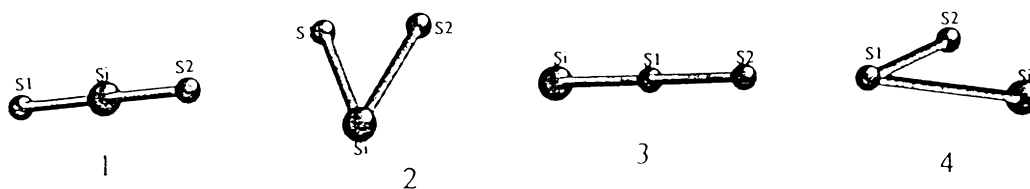* Corresponding author. Fax: +86-431-8923907.

Fig. 1. Geometrical structures of different $SiS_2^+$ isomers.

theoretical studies on binary clusters containing silicon. For example, Reiko Kishi et al. [6] investigated the geometries and energies of $Si_nF^-$ and $Si_nF$ ($n =$ 1–7) with ab initio MO calculations. Cangshan Xu et al. analyzed and assigned to various electronic states of $Si_nH$ and $Si_nH^-$, the ground state structures of anions and neutrals by ab initio calculations [7]; and Reiko Kishi et al. [8,9] studied the geometric and electronic structures of the mixed clusters $Si_nNa$, and $Si_nNa^-$ ($1 \leq n \leq 7$) with ab initio molecular orbital calculations; and Harkless et al. have calculated the structures and energies of $(SiO_2)_n$ clusters ($1 \leq n \leq$ 8) using the molecular dynamics simulation [10], Nayak et al. studied the atomic and electronic structures of neutral and charged $Si_nO_m$ clusters using density functional theory [11]. There are a lot of studies on Si–C clusters, such as Si doped in fullerene [12], the vibrational spectra of hexa-atomic silicon–carbon cluster $SiC_4Si$ [13] and so on.

Sulfur has the largest number of allotropes of any element. The study of the geometric and electronic structure of sulfur is very important in investigating properties and their applications. Much attention was paid for sulfur clusters and binary clusters, which contain sulfur. The ground state geometries of sulfur clusters $S_2$–$S_{13}$ have been calculated by Hohl et al. using a parameter-free density functional (DF) method, combined with molecular dynamics (MD) and simulated annealing techniques [14]. Raghavachari et al. explored the geometric structures and relative stability of small sulfur clusters ($S_2$–$S_{12}$) by means of ab initio quantum chemical calculations [15]. The experimental studies of binary clusters containing sulfur have been a focus; many new clusters have been synthesized, such as S–Ag [16,17], S–Au [16,17], S–Co [18], S–Fe [19], S–Ta [20], S–Mn [21], S–V [22] clusters and so on. However, theoretical studies on these clusters are quite limited. However there are many studies on S–C clusters,

especially about $CS_2$ monomer, dimer and $(CS_2)_n$ clusters [23–25].

Recently silicon–sulfur clusters $Si_mS_n$, anions and cations have been produced by us using direct laser ablation on a solid sample containing a mixture of sulfur and silicon powder, photodissociation of the clusters was studied with a tandem time-of-flight (TOF) mass spectrometer. There are many intense peaks of clusters anions and cations in the mass spectra, such as $(SiS_2)_n^{\pm}$, $[(SiS_2)_nS]^{\pm}$, $[(SiS_2)_nSiS]^+$, $[(SiS_2)_nSi_6S]^-$, $[(SiS_2)_nSi_6]^-$, and $(SiS_2)_n^+$ are the most intense peaks of them all. We also studied the mass spectra of their small mass clusters distribution and found that the peaks of $(SiS_2)_n^+$ ($n = 1$–2) also are the most intense ones. It indicated that $(SiS_2)_n^+$ clusters are the most stable clusters. In this paper we calculate $(SiS_2)_n^+$ ($n = 1$–5) clusters and predict the mechanism of the $(SiS_2)_n^+$ cluster forming.

## 2. Computational details

The geometric and electronic structures of $(SiS_2)_n^+$ cluster ions and the harmonic vibrational frequencies of the most stable isomer were studied. The standard three parameter Becke exchange function with the Lee, Yang, and Parr correlation function (DFT/ B3LYP) [26–28] and the standard 6-31G$^*$ basis set [29–33] available in GAUSSIAN94/DFT have been used.

## 3. Results and discussions

### 3.1. $SiS_2^+$

$SiS_2^+$ is the smallest unit and can be the building block for $(SiS_2)_n^+$ clusters. In Fig. 1, we give the possible geometries of the $SiS_2^+$ clusters, and we have optimized these structures in order to obtain the lowest

Table 1
Bond length, overlap population, Mulliken charge, total, relative and binding energy of $SiS_2^+$

| Structure | Symmetry | Bond length (nm) | Overlap population | Mulliken charge | Total energy (a.u.) | Relative energy (eV) | Binding energy (eV) |
|---|---|---|---|---|---|---|---|
| 1 | $D_{\infty h}$ | Si–S1 0.1968 | 0.4307 | Si 0.5439 | −1085.54080 | 0.0 | 3.38 |
|  |  |  |  | S 0.2280 |  |  |  |
| 2 | $C_{2v}$ | Si–S1 0.2060 | 0.2262 | Si 0.7142 | −1085.51253 | 0.77 | 2.61 |
|  |  |  |  | S 0.1429 |  |  |  |
| 3 | $C_{\infty v}$ | Si–S1 0.2033 | 0.2778 | Si 0.7475 | −1085.50633 | 0.94 | 2.44 |
|  |  | S1–S2 0.1998 | 0.0864 | S1 −0.0562 |  |  |  |
|  |  |  |  | S2 0.3087 |  |  |  |
| 4 | $C_s$ | Si–S1 0.2088 | 0.2314 | Si 0.7698 | −1085.51150 | 0.80 | 2.58 |
|  |  | S1–S2 0.2040 | 0.1105 | S1 −0.0203 |  |  |  |
|  |  |  |  | S2 0.2505 |  |  |  |

Table 2
Molecular orbitals and orbital energies of $(SiS_2)_n^+$ ($n = 1-5$)

| Cluster | Symmetry | State | Molecular orbital HOMO LUMO | Orbital energy (eV) HOMO LUMO | Energy gap (eV) | Orbital component HOMO LUMO |
|---|---|---|---|---|---|---|
| $SiS_2^+$ | $D_{\infty h}$ | $^2\Pi_g$ | $\pi_g$ <br> $\pi_g^*$ | $-13.95$ <br> $-12.37$ | 1.58 | $p_x(S)$ <br> $p_y(S)$ |
| $(SiS_2)_2^+$ | $D_{2h}$ | $^2B_{3g}$ | $b_{2u}$ <br> $b_{3g}$ | $-12.05$ <br> $-11.04$ | 1.01 | $p_y(S3,S4)$ <br> $p_y(S3,S4)$ |
| $(SiS_2)_3^+$ | $D_{2d}$ | | $e_g$ <br> $e_u$ | $-10.96$ <br> $-10.55$ | 0.41 | $p_y(S5)p_x(S6)$ <br> $p_y(S5)p_x(S6)$ |
| $(SiS_2)_4^+$ | $D_{2h}$ | $^2B_{2u}$ | $b_{1g}$ <br> $b_{2u}$ | $-10.46$ <br> $-10.10$ | 0.36 | $p_y(S7,S8)$ <br> $p_y(S7,S8)$ |
| $(SiS_2)_5^+$ | $D_{2d}$ | $^2A_2$ | $b_1$ <br> $b_2$ | $-10.44$ <br> $-10.18$ | 0.26 | $p_y(S3,S4)$ <br> $p_x(S9)P_y(S10)$ |

Table 3
Normal-mode vibrational frequencies ($cm^{-1}$) of $(SiS_2)_n^+$ ($n = 1-5$)

| $(SiS_2^+$ | $D_{\infty h}$ | $99/9(\pi_u)$[a] | $99/9(\pi_u)$ | $473/0.0(\sigma_g)$ | $596/194(\sigma_u)$ |
|---|---|---|---|---|---|
| $(SiS_2)_2^+$ | $D_{2h}$ | $49/1(b_{3u})$ | $108/4(b_{2u})$ | $150/0.0(b_{2g})$ | $158/0.0(b_{3g})$ |
| | | $228/8(b_{3u})$ | $242/0.0(a_g)$ | $318/260(b_{1u})$ | $424/3(b_{3g})$ |
| | | $456/4(a_g)$ | $508/886(b_{1u})$ | $607/75(b_{2u})$ | $263/0.0(a_g)$ |
| $(SiS_2)_3^+$ | $D_{2d}$ | $34/0(e)$ | $35/0(e)$ | $94/0.0(a)$ | $17/1(e)$ |
| | | $132/1(e)$ | $162/0.0(a)$ | $174/2(e)$ | $178/2(e)$ |
| | | $220/4(e)$ | $222/4(e)$ | $272/375(b_2)$ | $370/0.0(a)$ |
| | | $393/952(b_2)$ | $435/0(e)$ | $438/0(e)$ | $450/0.0(a)$ |
| | | $457/728(b_2)$ | $604/61(e)$ | $609/72(e)$ | $664/835(b2)$ |
| | | $730/0.0(a)$ | | | |
| $(SiS_2)_4^+$ | $D_{2h}$ | $22/0(b_{2u})$ | $25/0(b_{1u})$ | $41/0.0(b_{2g})$ | $68/0.0(a_u)$ |
| | | $108/0.0(b_{3g})$ | $111/0.0(b_{1g})$ | $122/0.0(a_g)$ | $137/5(b_{2u})$ |
| | | $137/0(b_{1u})$ | $171/0.0(b_{1g})$ | $183/0.0(b_{2g})$ | $211/1(b_{2u})$ |
| | | $216/9(b_{1u})$ | $228/0.0(b_{2g})$ | $229/46(b_{3u})$ | $318/0.0(a_g)$ |
| | | $354/281(b_{3u})$ | $411/0.0(a_g)$ | $424/0.0(b_{1g})$ | $430/414(b_{3u})$ |
| | | $433/1(b_{2u})$ | $446/0.0(b_{2g})$ | $449/0.0(a_g)$ | $459/868(b_{3u})$ |
| | | $595/51(b_{1u})$ | $596/0.0(a_g)$ | $608/0.0(b_{1g})$ | $610/145(b_{2u})$ |
| | | $679/1594(b_{3u})$ | $729/0.0(a_g)$ | | |
| $(SiS_2)_5^+$ | $D_{2d}$ | $14/1(e)$ | $14/1(e)$ | $36/0(e)$ | $36/0(e)$ |
| | | $57/0.0(b_1)$ | $94/0.0(a_1)$ | $103/0.0(a_2)$ | $119/1(e)$ |
| | | $119/(e)$ | $131/0.0(b_1)$ | $149/2(e)$ | $149/2(e)$ |
| | | $177/0(e)$ | $177/0(e)$ | $186/9(b_2)$ | $203/4(e)$ |
| | | $203/4(e)$ | $219/2(e)$ | $219/2(e)$ | $264/0.0(a_1)$ |
| | | $318/72(b_2)$ | $361/0.0(a_1)$ | $372/309(b_2)$ | $403/0.0(a_1)$ |
| | | $413/5(e)$ | $413/5(e)$ | $413/29(b_2)$ | $432/0.0(a_1)$ |
| | | $436/1(e)$ | $436/1(e)$ | $495/47(b_2)$ | $529/8(e)$ |
| | | $529/8(e)$ | $544/0.0(a_1)$ | $576/180(b_2)$ | $599/68(e)$ |
| | | $599/68(e)$ | $787/1307(b_2)$ | $793/0.0(a_1)$ | |

[a] Frequency/IR Inten. (symmetry), IR inten. in km/mol.
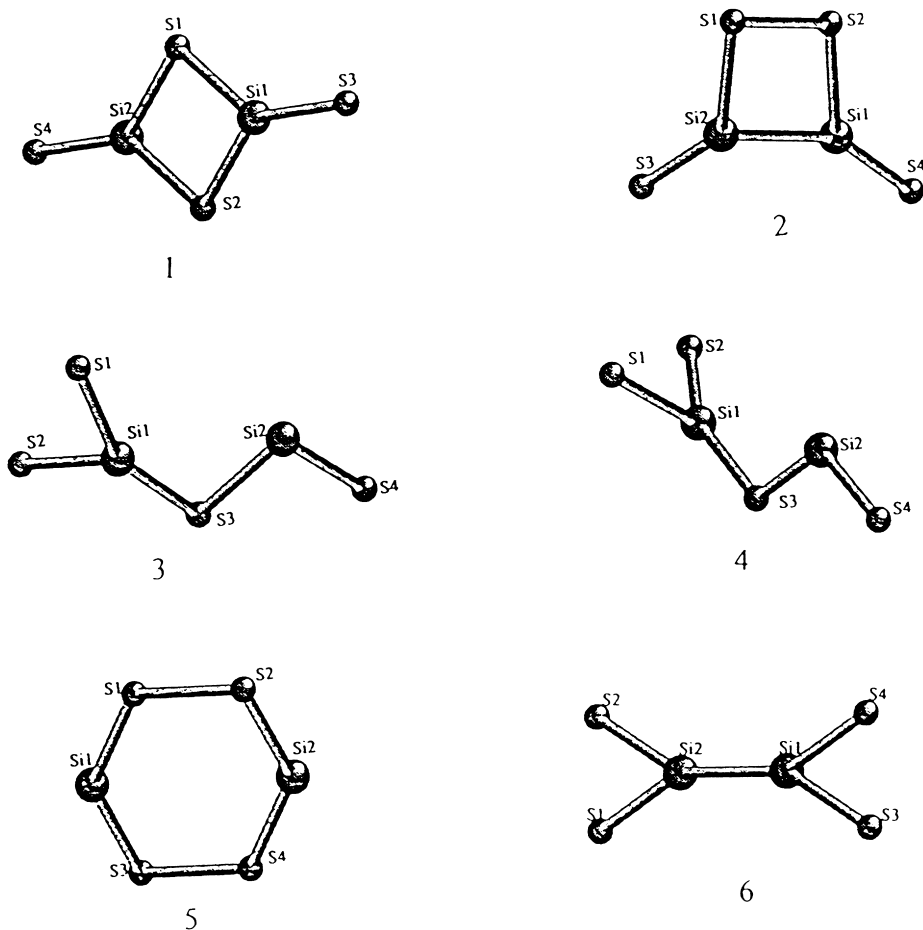
Fig. 2. Geometrical structures of different $(SiS_2)_2^+$ isomers.

energy structure. The parameters such as bond length, overlap population, Mulliken charge, total, relative, binding energy of different isomers are shown in Table 1: (1) is a linear structure with Si as the bridge of two S atoms, the symmetry is $D_{\infty h}$; (2) is a bent structure with Si as the bridge of two S atoms, the symmetry is $C_{2v}$; (3) is another linear structure with no Si as the bridge but with two S atoms bound together, the symmetry is $C_{\infty v}$; and (4) is yet another bent structure with no Si as the bridge but with two S atoms bound together and the symmetry is $C_s$. The relative energy order is $(1) < (2) < (4) < (3)$. The Si–S bond length is 0.1968 nm in structure (1), the overlap population is 0.4307, but in other structures, the Si–S bond lengths are all longer than 0.2 nm, and overlap population is less than 0.3. It is said that in the

structure with $D_{\infty h}$ symmetry, the overlap population between Si and S atoms is nearly twice that of other structures, so we predict that in the structure with $D_{\infty h}$ symmetry, the bond between Si and S atoms is a double bond. In the structures with $C_s$ and $C_{\infty v}$ symmetry, the overlap population on bonds S–S is 0.1105 and 0.0864, respectively, so the binding effects are very weak and the bonds are likely to break. We can predict that there is no S–S bond in the stable structures of $SiS_2^+$ This prediction can be proved by the study of vibrational frequency. Of the structure with $C_{\infty v}$ symmetry, there are imaginary frequencies, so the structure is not a stable structure of $SiS_2^+$.

Based on the optimized results, we analyze the electronic structure of the most stable structure of $SiS_2^+$ with the same method. The parameters are

Table 4
Bond length, overlap population, Mulliken charge, total, relative and binding energy of $(SiS_2)_2^+$

| Structure | Symmetry | Bond length (nm) | Overlap population | Mulliken charge | Total energy (a.u.) | Relative energy (eV) | Binding energy (eV) |
|---|---|---|---|---|---|---|---|
| 1 | $D_{2h}(1)$ | Si1–S1 0.2135 | 0.2115 | Si1 0.3990 | −2171.55956 | 0.0 | 19.77 |
| | | Si1–S3 0.1978 | 0.4855 | S1 0.0027 | | | |
| | | | | S3 0.0982 | | | |
| 2 | $C_{2v}$ | Si1–Si2 0.2392 | 0.1283 | Si1 0.2931 | −2171.50737 | 1.42 | 18.35 |
| | | Si1–S2 0.2290 | 0.1056 | S2 0.1387 | | | |
| | | Si1–S4 0.1933 | 0.5475 | S4 0.0682 | | | |
| | | S1–S2 0.2026 | 0.1669 | | | | |
| 3 | $C_s(1)$ | Si1–S1 0.2051 | 0.2175 | Si1 0.5652 | −2171.48780 | 1.95 | 17.82 |
| | | Si1–S2 0.2046 | 0.2222 | Si2 0.4421 | | | |
| | | Si1–S3 0.2039 | 0.3376 | S1 0.0465 | | | |
| | | Si2–S3 0.2350 | 0.0439 | S2 0.0636 | | | |
| | | Si2–S4 0.1981 | 0.4282 | S3 −0.1117 | | | |
| | | | | S4 −0.0058 | | | |
| 4 | $C_s(2)$ | Si1–S1 0.2047 | 0.2262 | Si1 0.5554 | −2171.48277 | 2.09 | 17.68 |
| | | Si1–S3 0.2046 | 0.3376 | Si2 0.4490 | | | |
| | | Si2–S3 0.2351 | 0.0450 | S1 0.0695 | | | |
| | | Si2–S4 0.1976 | 0.4266 | S3 −0.1391 | | | |
| | | | | S4 −0.0043 | | | |
| 5 | $D_{2h}(2)$ | Si1–S1 0.2066 | 0.3082 | Si1 0.5342 | −2171.46808 | 2.49 | 17.28 |
| | | S1–S2 0.2284 | 0.0264 | S1 −0.0171 | | | |
| 6 | $D_{2h}(3)$ | Si1–Si2 0.2212 | 0.2932 | Si1 0.4084 | −2171.42581 | 3.64 | 16.13 |
| | | Si1–S4 0.2064 | 0.2127 | S4 0.0458 | | | |
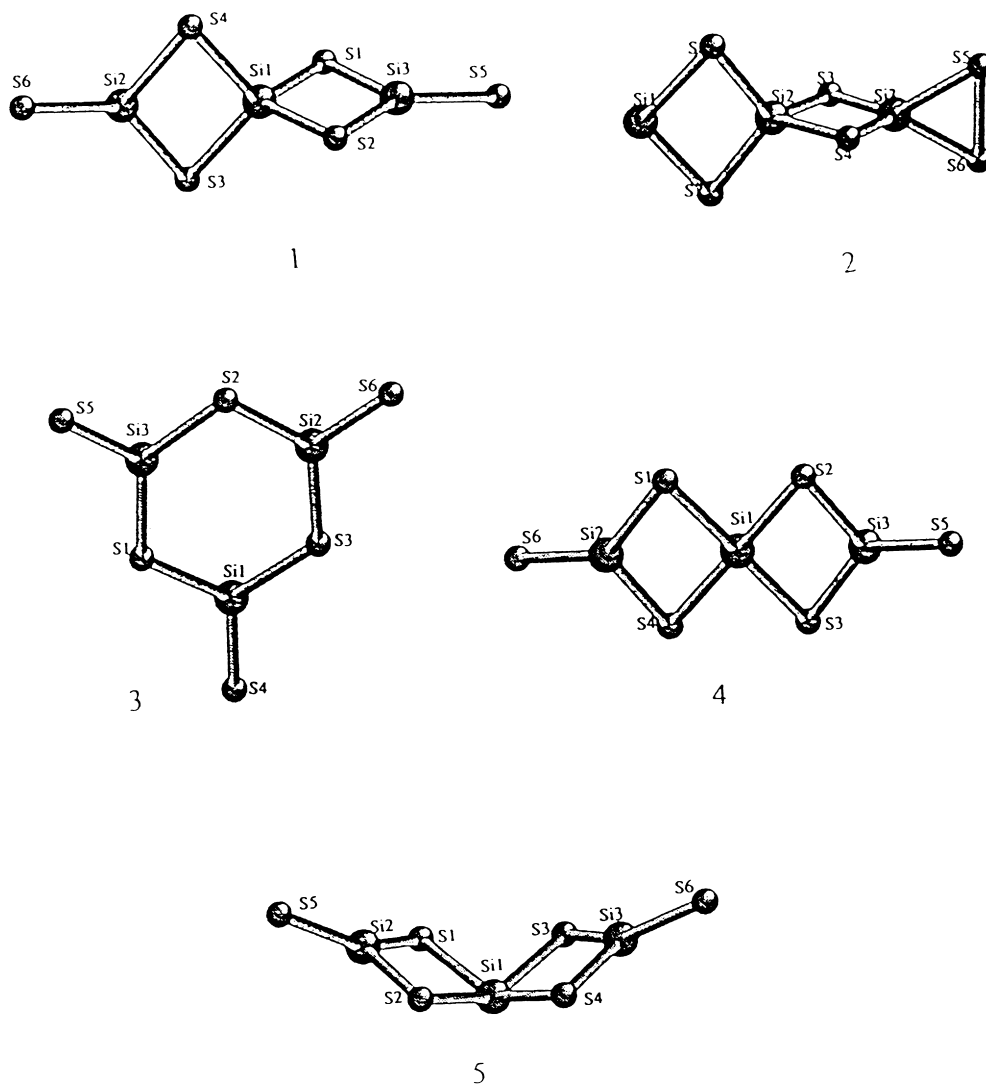
Fig. 3. Geometrical structures of different $(SiS_2)_3^+$ isomers.

shown in Table 2. The symmetry of the most stable structure of $SiS_2^+$ is $D_{\infty h}$, electronic state is $^2\Pi_g$ HOMO is $\pi_g$, the orbital energy is $-13.95$ eV, and its main component is $p_x$ orbital of S atoms. LUMO is $\pi_g^*$, the orbital energy is $-12.37$ eV, and its main component is $p_y$ orbital of S atoms.

The analysis of the frequency spectrum of the most stable structure of $SiS_2^+$ is shown in Table 3, the symmetry is $D_{\infty h}$, there are four spectral lines, three have infrared activity, the normal modes are of $\sigma_u^+$, $\pi_u$ symmetry. The strongest line (IR) is at 596 cm$^{-1}$, the

infrared intensity is 194.376 km/mol, the normal mode is of $\sigma_u^+$ symmetry and it is the stretching vibration of S atoms along the molecular axis.

### 3.2. $(SiS_2)_2^+$

$(SiS_2)_2^+$ can be regarded as the dimer of $SiS_2$ and $(SiS)_2^+$ with the chemical bonding of Si–S, Si–Si, S–S. The optimized structures of $(SiS_2)_2^+$ are displayed in Fig. 2, wherein: (1) is the planar structure with Si and S atoms bound together alternately,

Table 5
Bond length, overlap population, Mulliken charge, total, relative and binding energy of $(SiS_2)_3^+$

| Structure | Symmetry | Bond length (nm) | Overlap population | Mulliken charge | Total energy (a.u.) | Relative energy (eV) | Binding energy (eV) |
|---|---|---|---|---|---|---|---|
| 1 | $D_{2d}$ | Si1–S1 0.2186 | 0.2233 | Si1 0.1782 | −3257.56447 | 0.0 | 35.78 |
| | | Si3–S1 0.2117 | 0.2378 | Si3 0.4143 | | | |
| | | Si3–S5 0.1990 | 0.4838 | S1 −0.0200 | | | |
| | | | | S5 0.0366 | | | |
| 2 | $C_{2v}(1)$ | Si1–S1 0.2242 | 0.1339 | Si1 0.5050 | −3257.55767 | 0.19 | 35.59 |
| | | Si2–S1 0.2105 | 0.3136 | Si2 0.1908 | | | |
| | | Si2–S3 0.2230 | 0.1450 | Si3 0.3440 | | | |
| | | Si3–S3 0.2079 | 0.3187 | S1 −0.1559 | | | |
| | | Si3–S5 0.2183 | 0.1222 | S3 −0.0360 | | | |
| | | S5–S6 0.2080 | 0.0716 | S5 0.1700 | | | |
| 3 | $D_{3h}$ | Si1–S1 0.2137 | 0.1965 | Si1 0.3600 | −3257.51318 | 1.40 | 34.38 |
| | | Si1–S4 0.1968 | 0.5054 | S1 −0.0611 | | | |
| | | | | S4 0.0343 | | | |
| 4 | $D_{2h}$ | Si1–S1 0.2230 | 0.2359 | Si1 0.5479 | −3257.50517 | 1.61 | 34.17 |
| | | Si2–S1 0.2109 | 0.2356 | Si2 0.4036 | | | |
| | | Si2–S6 0.1982 | 0.4772 | S1 −0.1099 | | | |
| | | | | S6 0.0422 | | | |
| 5 | $C_{2v}(2)$ | Si1–S1 0.2338 | 0.1076 | Si1 0.4318 | −3257.43435 | 3.54 | 32.24 |
| | | Si2–S1 0.2103 | 0.2475 | S1 −0.0752 | | | |
| | | Si2–S5 0.1985 | 0.4509 | S5 0.0420 | | | |
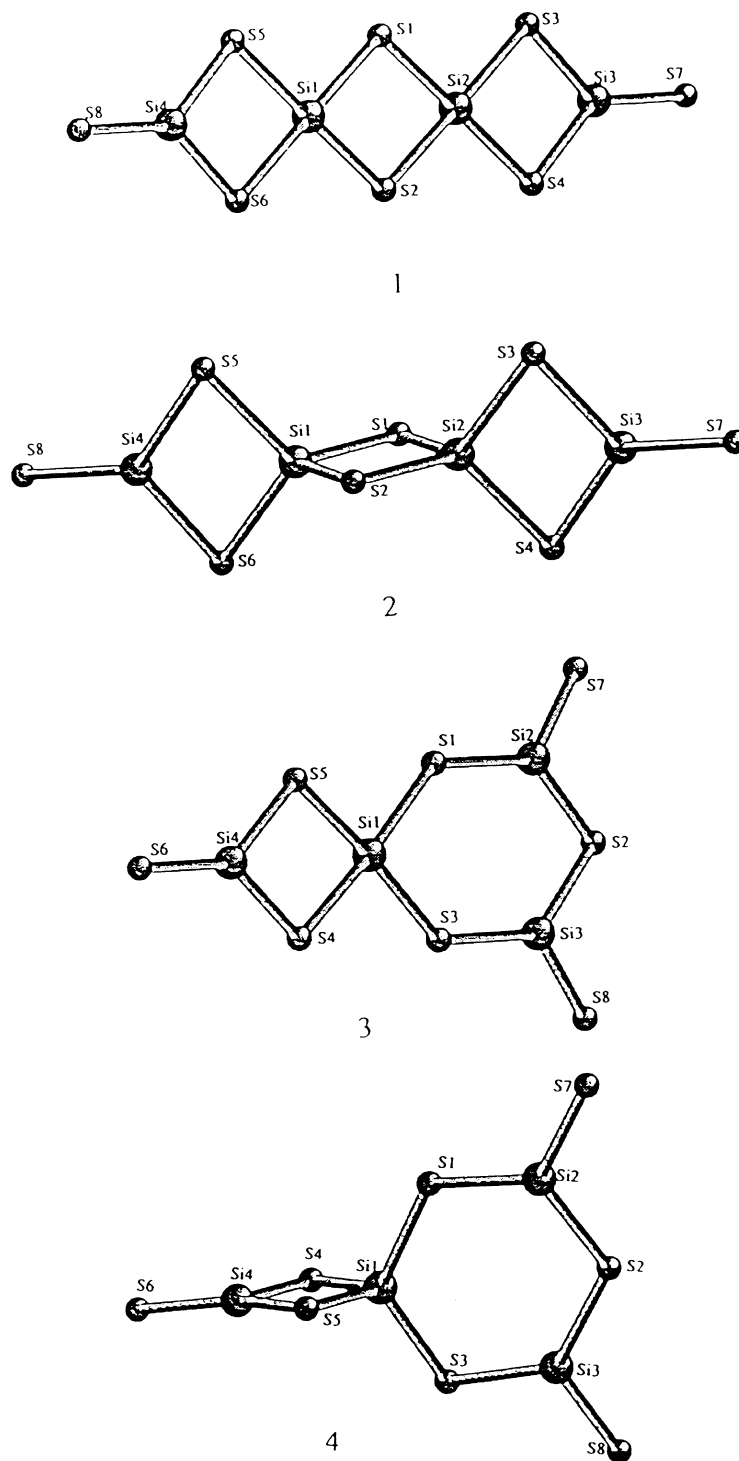
Fig. 4. Geometrical structures of different $(SiS_2)_4^+$ isomers.

forming a tetratomic ring, and the other two S atoms bonding to Si atoms, its symmetry is $D_{2h}$, denoted as $D_{2h}(1)$; (2) is a trapezoidal structure of planar tetratomic ring with the bonding of Si–Si, S–S, and the symmetry is $C_{2v}$; (3) is a planar branch structure with the bonding of Si–S, and its symmetry is $C_s$, denoted as $C_s(1)$; (4) is a three-dimensional branch structure with the bonding of Si–S, with the plane of $SiS_2$ perpendicular to the plane of $SiS_2^+$ and its symmetry is $C_s$ either, denoted as $C_s(2)$; (5) is a planar structure of hexatomic ring with the bonding of S–S, its symmetry also is $D_{2h}$, denoted as $D_{2h}(2)$; (6) is a planar structure with the bonding of Si–Si which like ethylene, its symmetry is $D_{2h}$, denoted as $D_{2h}(3)$. The parameters of bond length, overlap population, Mulliken charge, total, relative and binding energy are shown in Table 4. The relative energy order is obtained as (1) < (2) < (3) < (4) < (5) < (6). While the structures of dimer with Si–S bond are stable, the structures only with the bond of Si–Si, S–S are not stable. The vibrational spectra can prove this conclusion, because there are imaginary frequencies in the structures of (5) and (6). In the structure with $D_{2h}(1)$, the bond length of Si1–S1 is 0.2135 nm, the bond length of Si1–S3 is 0.1978 nm, and overlap population of them are 0.2115 and 0.4855, respectively. It can be inferred that in the stable structure of $(SiS_2)_2^+$, the bond of the Si–S of the ring is a single bond, and the external Si–S bond is a double bond. There is a negative charge on S atoms in $SiS_2$, and a large amount of positive charge on the Si atom of $SiS_2^+$ so $SiS_2$ and $SiS_2^+$ can combine together and form a tetratomic ring structure with the bonding of Si–S.

The symmetry of the most stable structure of $(SiS_2)_2^+$ is $D_{2h}$ (Table 2), electronic state is $^2B_{3g}$. HOMO is $b_{2u}$ orbital, and its energy is $-12.05$ eV, and its main component is $p_y$ of S3, S4. LUMO is the $b_{3g}$ orbital, its energy is $-11.04$ eV, and its main component is $p_y$ of S3, S4 either.

There are twelve spectral lines in the vibrational spectrum of the most stable structure with $D_{2h}$ symmetry (Table 3). Six of them have infrared activity, their vibrational modes are of $b_{1u}$, $b_{2u}$, $b_{3u}$ symmetry. The strongest line (IR) is at 508 cm$^{-1}$, the infrared intensity is 886.268 km/mol, and symmetry of the normal mode is $b_{1u}$. It is the stretching vibration of S3, S4 atoms along the molecular axis.

### 3.3. $(SiS_2)_3^+$

We designed the structures of the trimer based on the dimers, that is, the bonding of Si–S is the main binding effect among monomers. The structures are shown in Fig. 3: (1) is a three-dimensional structure with two tetratomic rings perpendicular to each other, its symmetry is $D_{2d}$; (2) also is a three-dimensional structure with two tetratomic rings and a tri-atomic ring perpendicular to each other, its symmetry is $C_{2v}$, denoted as $C_{2v}(1)$; (3) is a planar structure of a hexatomic ring with a symmetry of $D_{3h}$; (4) is a planar structure of two tetratomic rings with a symmetry of $D_{2h}$; (5) is a three-dimensional structure with two tetratomic ring having an angle, its symmetry is also $C_{2v}$, denoted $C_{2v}(2)$. The structures are optimized and the parameters are shown in Table 5. The relative energy order is obtained as (1) < (2) < (3) < (4) < (5). We found that trimer trends have a tetratomic ring structure with the rings perpendicular to each other; than having a hexatomic ring structure. There is a large repelling effect between S atoms in the structures with the symmetry of $D_{2h}$ and $C_{2v}(2)$, so they are unstable towards the other structures whose rings are perpendicular to each other.

The symmetry of the most stable structure of $(SiS_2)_3^+$ is $D_{2d}$ (Table 2). HOMO of $(SiS_2)_3^+$ is $e_g$ orbital, and its energy is $-10.96$ eV, its main component is $p_y$ of S5 and $p_x$ of S6. LUMO is $e_u$ orbital, its energy is $-10.55$ eV, and its main component is $p_y$ of S5 and $p_x$ of S6, either.

There are twenty-one spectral lines in the vibrational spectrum of the most stable structure with $D_{2d}$ symmetry of $(SiS_2)_3^+$ (Table 3). Sixteen of them have infrared activity, the symmetry of their vibrational modes are e, $b_2$. The strongest line (IR) is at 393 cm$^{-1}$, the infrared intensity is 952.310 km/mol, the symmetry of the normal mode is $b_2$, they are the stretching vibration of S5, S6 atoms along the molecular axis and the twisting vibration of S1–S4 in the molecular plane.

### 3.4. $(SiS_2)_4^+$

The optimized geometrical structures of $(SiS_2)_4^+$ are displayed in Fig. 4, and the parameters are shown in Table 6: (1) is a planar structure of three tetra-atomic rings with a symmetry of $D_{2h}$, denoted as $D_{2h}(1)$; (2) is

Table 6
Bond length, overlap population, Mulliken charge, total, relative and binding energy of $(SiS_2)_4^+$

| Structure | Symmetry | Bond length (nm) | Overlap population | Mulliken charge | Total energy (a.u.) | Relative energy (eV) | Binding energy (eV) |
|---|---|---|---|---|---|---|---|
| 1 | $D_{2h}(1)$ | Si1–S1 0.2195 | 0.2605 | Si1 0.5550 | −4343.44671 | 3.31 | 48.45 |
| | | Si1–S5 0.2240 | 0.2304 | Si4 0.3950 | | | |
| | | Si4–S5 0.2106 | 0.2342 | S1 −0.22076 | | | |
| | | Si4–S8 0.1983 | 0.4784 | S5 −0.1252 | | | |
| | | | | S8 0.0082 | | | |
| 2 | $D_{2h}(2)$ | Si1–S1 0.2149 | 0.2445 | Si1 0.2189 | −4343.56827 | 0.0 | 51.76 |
| | | Si1–S5 0.2118 | 0.2343 | Si4 0.4115 | | | |
| | | Si4–S5 0.2111 | 0.2343 | S1 −0.0447 | | | |
| | | Si4–S8 0.1991 | 0.2450 | S5 −0.0467 | | | |
| | | | 0.4827 | S8 0.0076 | | | |
| 3 | $C_{2v}(1)$ | Si1–S1 0.2250 | 0.1847 | Si1 0.6083 | −4343.44397 | 3.38 | 48.38 |
| | | Si1–S4 0.2213 | 0.2515 | | | | |
| | | Si2–S1 0.2109 | 0.2299 | Si2 0.3701 | | | |
| | | Si2–S2 0.2131 | 0.1994 | Si4 0.3721 | | | |
| | | Si2–S7 0.1979 | 0.5015 | S1 −0.2022 | | | |
| | | Si4–S4 0.2129 | 0.2104 | S2 −0.0640 | | | |
| | | Si4–S6 0.1957 | 0.5247 | S4 −0.1224 | | | |
| | | | | S6 −0.0289 | | | |
| | | | | S7 0.0107 | | | |
| 4 | $C_{2v}(2)$ | Si1–S1 0.2187 | 0.1319 | Si1 0.1133 | −4343.51054 | 1.57 | 50.19 |
| | | Si1–S4 0.2146 | 0.2511 | Si2 0.3818 | | | |
| | | Si2–S1 0.2100 | 0.2601 | Si4 0.3729x | | | |
| | | Si2–S2 0.2137 | 0.2040 | Si4 0.3729 | | | |
| | | Si2–S7 0.1982 | 0.4883 | S1 −0.0589 | | | |
| | | Si4–S4 0.2149 | 0.2022 | S2 −0.0732 | | | |
| | | Si4–S6 0.1953 | 0.5574 | S4 −0.0223 | | | |
| | | | | S6 −0.0502 | | | |
| | | | | S7 0.0181 | | | |
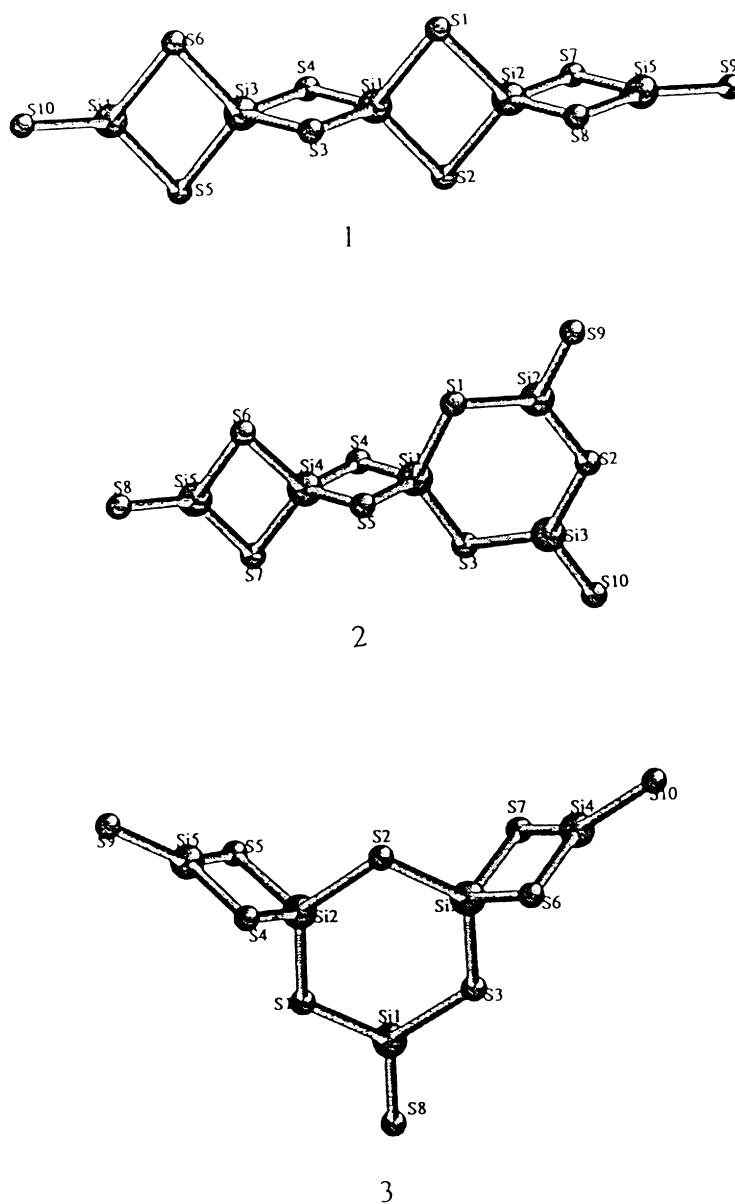
Fig. 5. Geometrical structures of different $(SiS_2)_5^+$ isomers.

a three-dimensional structure with three tetra-atomic ring perpendicular to each other, the symmetry is also $D_{2h}$, denoted as $D_{2h}$ (2); (3) is a planar structure with a hexatomic ring and a tetra-atomic ring, its symmetry is $C_{2v}$, denoted as $C_{2v}$ (1); and (4) is a three-dimensional structure with a hexatomic ring and a tetra-atomic ring perpendicular to each other, its symmetry is also $C_{2v}$, denoted as $C_{2v}$ (2). The relative energy order is (2) < (4) < (3) < (1). The difference between (1), (3), (2), and (4) is that the rings in the first two structures are in the same plane, while the rings in the latter are perpendicular to each other. It indicates that if Si atoms and S atoms bond to the Si atoms are in the same plane, there will be a large

Table 7
Table 7
Bond length, overlap population, Mulliken charge, total, relative and binding energy of $(SiS_2)_5^+$

| Structure | Symmetry | Bond length (nm) | Overlap population | Mulliken charge | Total energy (a.u.) | Relative energy (eV) | Binding energy (eV) |
|---|---|---|---|---|---|---|---|
| 1 | $D_{2d}$ | Si1–S1 0.2150 | 0.2516 | Si1 0.2286 | −5429.55054 | 0.0 | 67.15 |
| | | Si2–S1 0.2174 | 0.2097 | Si2 0.2016 | | | |
| | | Si2–S7 0.2137 | 0.2677 | Si5 0.3521 | | | |
| | | Si5–S7 0.2171 | 0.1851 | S1 −0.0010 | | | |
| | | Si5–S9 0.1935 | 0.5995 | S2 −0.0417 | | | |
| | | | | S9 −0.0821 | | | |
| 2 | $C_{2v}(1)$ | Si1–S1 0.2178 | 0.1852 | Si1 0.1619 | −5429.51252 | 1.03 | 66.12 |
| | | Si1–S4 0.2151 | 0.2529 | Si2 0.3671 | | | |
| | | Si2–S1 0.2110 | 0.2425 | Si4 0.2413 | | | |
| | | Si2–S2 0.2137 | 0.2037 | Si5 0.3961 | | | |
| | | Si2–S9 0.1973 | 0.5128 | S1 −0.0814 | | | |
| | | Si4–S4 0.2155 | 0.2367 | S2 −0.0837 | | | |
| | | Si4–S6 0.2171 | 0.2515 | S4 −0.0392 | | | |
| | | Si5–S6 0.2120 | 0.2323 | S6 −0.0614 | | | |
| | | Si5–S8 0.1978 | 0.5107 | S8 −0.0322 | | | |
| | | | | S9 −0.0268 | | | |
| 3 | $C_{2v}(2)$ | Si1–S1 0.2142 | 0.1965 | Si1 0.3407 | −5429.50536 | 1.23 | 65.92 |
| | | Si1–S8 0.1942 | 0.5871 | Si2 0.1281 | | | |
| | | Si2–S1 0.2137 | 0.1953 | Si5 0.4230 | | | |
| | | Si2–S2 0.2146 | 0.1896 | S1 −0.0773 | | | |
| | | Si2–S4 0.2193 | 0.2278 | S2 −0.0741 | | | |
| | | Si5–S4 0.2106 | 0.2497 | S4 −0.0305 | | | |
| | | Si5–S9 0.1995 | 0.4705 | S8 −0.0928 | | | |
| | | | | S9 0.0002 | | | |

repelling effect between S atoms, so the structures will be unstable. Comparing the bond length and the overlap population, the bonds of Si–S in structures (3) and (1) are longer than those in structures (2) and (4), and the overlap population is less. There are great differences of total energy, so we conclude that structures (2) and (4) are more stable than structures (1) and (3). However, (4) has an imaginary frequency, so (2) is the most stable structure.

The symmetry of the most stable structure of $(SiS_2)_4^+$ is $D_{2h}$ (Table 2), its electronic state is $^2B_{2u}$. HOMO is the $b_{1g}$ orbital, and its energy is $-10.46$ eV, its main component is $p_y$ of S7, S8. LUMO is the $b_{2u}$ orbital, its energy is $-10.10$ eV, and its main component is $p_y$ of S7 and S8 either.

There are thirty spectral lines in the vibrational spectrum of the most stable structure of $(SiS_2)_4^+$ with $D_{2h}$ symmetry (Table 3). Fifteen of them have infrared activity, the symmetries of their vibrational modes are $b_{1u}, b_{2u}, b_{3u}$. The strongest line (IR) is at $679$ cm$^{-1}$, the infrared intensity is 1593.840 km/mole, the symmetry of the normal mode is $b_{3u}$, and it is the stretching vibration of Si atoms and S7, S8 atoms along the molecular axis.

### 3.5. $(SiS_2)_5^+$

Based on the conclusions from geometric characters of tetramers, we designed the geometric structures of the $(SiS_2)_5^+$ pentamer. The optimized structures are displayed in Fig. 5. The geometric character of these structures is that the monomers bond together with the tetratomic and hexatomic rings perpendicular to each other. The parameters are shown in Table 7: (1) is a structure of $D_{2d}$ symmetry with four tetratomic rings perpendicular to each other; (2) with two tetratomic rings perpendicular to each other and then perpendicular to a hexatomic ring, its symmetry is $C_{2v}$, denoted as $C_{2v}$ (1); and (3) with two tetratomic rings perpendicular to a hexatomic ring, respectively, its symmetry is also $C_{2v}$, denoted as $C_{2v}$ (2). The relative energy order is obtained as (1) < (2) < (3). In the structures with hexatomic rings, the Si–S bond is longer than that in the structure with tetratomic rings, and the overlap population is also less. The structures with tetratomic rings are more stable than the structures with hexatomic rings.

The most stable structure of $(SiS_2)_5^+$ is of $D_{2d}$

symmetry (Table 2), and its electronic state is $^2A_2$. Its HOMO is $b_1$ orbital, its energy is $-10.43$ eV, and its main component are $p_x$ and $p_y$ orbitals of S atoms. Its LUMO is the $b_2$ orbital, its energy is $-10.18$ eV, and its main component are $p$ orbitals of S atoms.

There are thirty-nine spectral lines in the vibrational spectrum of the most stable structure of $(SiS_2)_5^+$ with $D_{2d}$ symmetry (Table 3). Twenty-nine of them have infrared activity and the symmetries of their vibrational modes are $e, b_2$. The strongest line (IR) is at $787$ cm$^{-1}$, the infrared intensity is 1306.893 km/mol, the normal mode is $b_2$ symmetry, and it is the stretching vibration of Si4 and Si5 atoms and S9, S10 atoms along the molecular axis.

## 4. Conclusions

1. The most stable structures of $SiS_2^+$ is with $D_{\infty h}$ symmetry, and $(SiS_2)_n^+$ ($n = 2$–$5$) have tetraatomic rings of Si and S atoms bonded alternatively, and the rings are perpendicular to each other.
2. It is predicted that the growing trend of $(SiS_2)_n^+$ based on the bonding of Si and S atoms with $SiS_2^+$ as the core and $SiS_2$ as the building block, forming tetratomic ring molecular chains with rings perpendicular to each other.
3. From the component of the most stable structure molecular orbitals, one can notice that all the HOMO and LUMO orbitals are formed by $p$ atomic orbitals of S atoms, the energy values of HOMO and LUMO are all negative, and the energy gap decreases as the length of the molecular chain increases. So the stability of the molecules decreases as the length of the molecular chain increases.

## References

[1] H.W. Kroto, J.R. Heath, S.C. O'Brier, R.F. Curl, R.E. Smalley, Nature 318 (1985) 162.
[2] Ji-Kang Feng, Chin. J. Org. Chem. 12 (1992) 567.

[3] Ji-Kang Feng, Chin. J. Org. Chem. 13 (1993) 25.

[4] K. Raghavachari, J. Chem. Phys. 84 (1986) 5672.

[5] C.M. Rohlfing, Raghavachari, J. Chem. Phys. 96 (1992) 2114.

[6] Reiko Kishi, Yuichi Negishi, Hiroshi Kawamata, et al., J. Chem. Phys. 108 (1998) 8039.

[7] Cangshan Xu, T.R. Taylor, G.R. Burton, D.M. Neumark, J. Chem. Phys. 108 (1998) 7645.

[8] Reiko Kishi, Suehiro Lwata, Atsushi Nakajima, Koji Kaya, J. Chem. Phys. 107 (1997) 3056.

[9] Reiko Kishi, Hiroshi Kawamata, Yuichi Negishi, et al., J. Chem. Phys. 107 (1997) 10 029.

[10] J.A. Harkless, D.K. Stillinger, F.H. Stillinger, J. Phys. Chem. 100 (1996) 1098.

[11] S.K. Nayak, B.K. Rao, S.N. Khanna, P. Jena, J. Chem. Phys. 109 (1998) 1245.

[12] J.L. Fye, M.F. Jarrold, J. Phys. Chem. 101 (1997) 1836.

[13] J.D. Presilla-Marquez, C.M.L. Rittby, W.R.M. Graham, J. Chem. Phys. 107 (1997) 8367.

[14] D. Hohl, R.O. Jones, R. Car, M. Parrinello, J. Chem. Phys. 89 (1988) 6823.

[15] K. Raghavachari, C.M. Rohlfing, J.S. Binkley, J. Chem. Phys. 93 (1990) 5862.

[16] Wei-Jie Huang, Zhao-Yang Liu, Rong-Bin Hang, Lan-Sun Zang, Acta Chimica Sinica 56 (1998) 200 (in Chinese).

[17] Bi-Xian Peng, Zhen Gao, Fanao Kong, et al., Chin. Sci., Ser. B 27 (1997) 221.

[18] Yang Shi, Nan Zhang, Zhen Gao, Fanao Kong, Qihe Zhu, J. Chem. Phys. 101 (1994) 9528.

[19] Zhong De Yu, Nan Zhang, Xiaojun Wu, Zhen Gao, Qihe Zhu, Fanao Kong, J. Chem. Phys. 99 (1993) 1765.

[20] Nan Zhang, Zhongde Yu, Xiaojun Wu, Zhen Gao, Qihe Zhu, Fanao Kong, J. Chem. Soc. Faraday Trans. 89 (1993) 1779.

[21] Yang Shi, Nan Zhang, Zhen Gao, Fanao Kong, Qihe Zhu, Chemistry 8 (1993) 27 (in Chinese).

[22] Wenjing Wang, Peng Liu, Dongbo Hu, Zhen Gao, Fanao Kong, Qihe Zhu, Chin. J. Chem. Phys. 10 (1997) 110 (in Chinese).

[23] M. Hochlaf, G. Chambaud, P. Rosmus, J. Chem. Phys. 108 (1998) 4047.

[24] A. Sanov, W.C. Lineberger, K.D. Jordan, J. Phys. Chem. 102 (1998) 2509.

[25] Toshihiko Maeyama, Takanobu Oikawa, Tohru Tsumura, Naohiko Mikami, J. Chem. Phys. 108 (1998) 1368.

[26] P.J. Hay, W.R. Wadt, J. Chem. Phys. 82 (1985) 270.

[27] W.R. Wadt, P.J. Hay, J. Chem. Phys. 82 (1985) 284.

[28] P.J. Hay, W.R. Wadt, J. Chem. Phys. 82 (1985) 299.

[29] R. Ditchfield, W.J. Hehre, J.A. Pople, J. Chem. Phys. 54 (1971) 724.

[30] W.J. Hehre, R. Ditchfield, J.A. Pople, J. Chem. Phys. 56 (1972) 2257.

[31] P.C. Hariharan, J.A. Pople, Theo. Chim. Acta. 28 (1973) 213.

[32] M.S. Gordon, Chem. Phys. 76 (1980) 163.

[33] P.C. Hariharan, J.A. Pople, Mol. Phys. (1974) 209.